JJEES

Volume 2, (Special Publication, Number 1), December. 2009
ISSN 1995-6681
Pages 108- 119

Jordan Journal of Earth and Environmental Sciences

Adsorption of Thorium (IV) and Uranium (VI) by Tulul al-Shabba Zeolitic Tuff, Jordan

Mona Al-Shaybe and Fawwaz Khalili*

University of Jordan, Chemistry Department, Amman – Jordan

Abstract

Tulul al-Shabba zeolite from Jordan was employed to remove actinides metal ions namely Uranium (VI) and Thorium (IV). The used Jordanian zeolitic tuff is dominated by phillipsite and chabazite. The sorption behavior of the used zeolitic tuff towards Th^{4+} and UO_2^{2+} metal(s) ions in aqueous solutions was studied by batch experiment as a function of pH, contact time and temperature and column techniques at 25.0°C and pH= 3. High initial rate of metal ions uptake was observed after 24 hr of shaking, and the uptake have increased with increasing pH and have reached a maximum at pH = 3. Tulul al-Shabba zeolitic tuff has shown high metal ion uptake capacity toward Thorium (IV) than Uranium (VI). Adsorption data was evaluated according to the Pseudo second-order reaction kinetic.

Adsorption isotherms were studied at temperature 25C°, 35C° and 45C°. The Langmuir, Freundlich and Dubinin-Raduskevich (D-R) adsorption models equations were applied, and the proper constants were derived. It was found that the adsorptivity process is enthalpy driven for Thorium (IV) and Uranium (VI).

Recovery of Thorium (IV) and Uranium (VI) ions after adsorption was carried out by treatment of the loaded zeolitic tuff in the column with 0.1N HNO_3, 0.1N H_2SO_4, 0.1 - 1*10 $^{-4}$N EDTA, and 0.1N sodium acetate. The best percent recovery for Thorium (IV) was obtained when 1*10^{-4}N EDTA was used, while for Uranium (VI) when 0.1N H_2SO_4 was used.

Keywords Jordanian zeolitic tuff, Thorium (IV), Uranium (VI), adsorption, isotherm, kinetic, recovery.

1. Introduction

Jordan is rich in industrial rocks and minerals. Zeolitic tuff is widely distributed in Jordan (Khoury et al., 2003). The huge reserves of the zeolitic tuff have encouraged the authors to carry out this work since investment projects of radioactive minerals have a priority in Jordan. Uranium is enriched in the Phosphorite and Chalk Marl Units of central Jordan (Daba-Siwaqa area 60 km south of Amman). The area is currently under investigation by Areva Co., and huge reserves are expected. UO_2 concentrations range between 140 – 2200 ppm in central Jordan. Thorium is associated with the Dubaydib Sandstone Formation, southern Jordan, where the level of thorium oxide reaches 400 ppm (Khoury, 2006).

The methods for separation, collection and detection of radionuclides are similar to ordinary analytical procedures and employ many of the chemical and physical principles that apply to the non-radioactive nuclides. However, some important aspects of the behavior of radionuclides are significantly different, resulting in challenges to the radio chemists to find means for isolation of a pure sample for analysis. There are many methods for the separation and purification of radionuclides. The oldest method, used in the large-scale separation of actinides, is the precipitation technique. However, this process produces complex products and impure substances.

Many ion-exchange separations of radionuclides are based on the formation of complex species between the metal and an extractant in the organic phase as in the extraction of Europium (III), Thorium(IV) and Uranium(VI) with didodecylphosphoric acid (HDDPA), (Kondo et al.1989); (Nazzal, 2006); (Khaled and Khalili, 1999). The use of solids for removing substances from either gaseous or liquid solution has been widely used since biblical times. This process, known as adsorption, involves nothing more than the preferential partitioning of substances from the gaseous or liquid phase onto the surface of solid substrate. From the early days of using bone char for decolorization of sugar solutions and other foods to the later implementation of activated carbon for removing nerve gases from the battlefield and to today's thousands of applications, the adsorption phenomenon has become a useful tool for purification and separation (Slejko, 1985 and Lazaridis et al., 2004).

Ion exchange is a process by which ions held in a porous, essentially insoluble solid exchange for ions in a solution that is brought in contact with solid. The ion exchange properties of clays and zeolite have been recognized and studied for more than a century (Skoog et al.1994); (Harvey, 2000). The main advantages of ion exchange over chemical precipitation are removal of metal value, selectivity, and less sludge volume produced-meeting the strict discharge specifications. In ion exchange system, polymeric resins as well as zeolite are usually

* Corresponding author. fkhalili@ju.edu.jo

employed. The availability of natural zeolite in many countries provides low-cost treatment by ion exchange systems (Ali and El-bishtawi, 1997).

The adsorption of Thorium (IV) and Uranium (VI) by zeolite isolated from Metaxades (Greece), using batch type method, was studied by Misaelides et al. (2006). They found that NaCl pretreated zeolite material improved the thorium uptake but not the uranium; this can be attributed to the improvement of the ion-exchange properties of the microporous minerals (Misaelides et al. 1995). The adsorption behavior of Th(IV) onto the PAN (Polyacrylonitrile)/zeolite, zeolite isolated from Manisa-Gordes (Turky), composite adsorbent was investigated. It was found that PAN (Polyacrylonitrile)/zeolite composite adsorbent is economical and an effective sorbent for Th(IV) ions, and the composite adsorbent exhibited an excellent adsorption selectivity for Th(IV) (Kaygun and Akyil, 2007).

The following work aims at studying the adsorption behavior of uranium and thorium by using the zeolitic tuff from Tulul Alshahba of Jordan. The batch technique of removing uranium and thorium from solution was carried out at specific conditions: pH= 1.0, 2.0, and 3.0, at temperatures 25.0°C, 35.0°C and 45.0°C at different contact time (kinetic) and with the same ionic strength (0.1M NaClO4). The column experiment was carried out at 25.0°C and pH= 3. Analysis of data will be based on adsorption models such as Langmuir, Freundlich and Dubinin–Radushkevich (D–R). Adsorption kinetics was applied in order to determine adsorption mechanism and adsorption characteristic constants. The effective adsorption from column and the coefficient of recovery with different ligands was studied for the adsorbed metal ions on the zeolitic tuff.

2. Methodology

2.1. Materials and Instrumentation

All reagents used in this study were analytical grade. $Th(NO_3)_4.5H_2O$ is from Riedel DeHäen Chemical company Inc, $UO_2(NO_3)_3.H_2O$, sodium perchlorate, sodium acetate, sulfuric acid and nitric acid are from Merck, EDTA is from PARK, 35% Hydrochloric acid from analytical Rasayan, Arsenazo (III) Indicator from BDH Chemicals Ltd. Infrared spectra of the zeolitic tuff was recorded using a Thermo Nicolet Nexus 870 FTIR. The thermal gravimetric analysis (TGA) of the zeolitic tuff was studied using NETZSCH STA 409 PC. The main and minor composition of zeolitic tuff was studied by X-ray powdered diffraction method (Shimadzu PXRD-6000). A pH meter model Cyberscan waterproof PC 300 was used for pH measurements. The analytical balance that was used is Shimadzu and its type is AW120, and its readability is 0.1 mg. Shaking of samples was done by using Clifton Shaker equipped with a thermostat. UV-VIS Spectrophotometer was from Spectroscan model 80DV with software UV Win5 v5.0.5.

2.2. Zeolitic tuff preparation.

Zeolitic tuff samples have a particle size of (250-500 µm) were chosen for this study. The zeolitic tuffs samples were converted to Na - type, by adding a 250 ml of 2M NaCl to each 200g of zeolitic tuff, and shaking for 24hr. The exchangeable cations in the zeolitic tuff structure were replaced by Na^+ ions. After shaking, the zeolitic tuff samples were washed several times with deionized water to get rid of excess NaCl. The samples were dried in an oven at 100°C overnight.

2.3. Specrophotometeric procedure for Thorium (IV) and Uranium(VI).

2.3.1. Preparation of Arsenazo (III) indicator solution.

A 0.10% aqueous solution of Arsenazo (III) was used as a spectrophotometric reagent in the determination of Thorium(IV) and Uranium(VI) ion concentration (Savvinn, 1961); (Khalili et al., 2008).

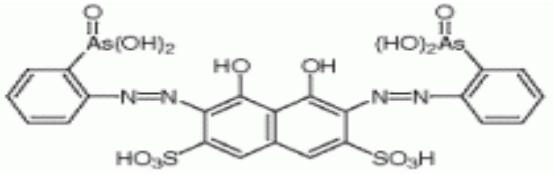

The spectrophotometric determination of Thorium (IV) and Uranium (VI) ions in the aqueous solution was carried out as follows:

Transfer 0.5 ml of Arsenazo (III) indicator to a 10 ml of 9.0 M Hydrochloric acid solution, and add 1.5 ml of the aqueous Thorium (IV) test solution or 2.0 ml in the case of Uranium (VI). Dilute the volume to 25.0 ml by addition of water. Absorption measurement was carried out using a (1.0 cm) quartz cell within one hour of sample preparation at 660 nm wavelength for Thorium (IV) and 650 nm wavelength for Uranium (VI).

2.4. Adsorption experiments

2.4.1. Metal ion-uptake by zeolitic tuff using batch adsorption.

Batch adsorption was carried out using Pyrex glass flasks. Experiments for determination the equilibrium time for the adsorption process involving 0.05 g ± 0.1 mg of the zeolitic tuff, 50.0 ml of metal ion was then added, and the mixed solutions were mechanically shaken. The contact time was varied from 0.25 hour to 24 hours at 25 °C, the concentration of the metal ion remaining was determined with UV- VIS. Similar experiments were also carried out at different pH 1.0, 2.0 and 3.0.

The mass of the adsorbed metal per unit mass of the zeolitic tuff was calculated using equation (1).

$$q = (C_i - C_e) * V / m \quad (1)$$

(Fendorf and Li, 1996; Lee et al., 2000).

q: Metal ion uptake by zeolitic tuff in (mg M / g zeolitic tuff).

C_i: Initial metal concentration (ppm).

C_e: The residual concentration of metal ion in solution at equilibrium in (ppm).

m: Mass of zeolitic tuff (g).

The percentage of metal ion loading by zeolitic tuff expressed as percentage uptake was calculated (Eq. (2)) where

$$\% \text{ Metal uptake} = C_e / C_i * 100 \quad (2)$$

$K_d = [(C_i - C_f) / C_i]\ V / m \quad (mL / g)$ (3)

Calculations were made by using these data, and adsorption curves were obtained.

2.5. Adsorption isotherm studies.

An accurate mass of 0.05 g of zeolitic tuff measured to the nearest 0.1 mg was shaken with 50.0 ml of metal ion solution at different concentrations, in a thermostatted shaker for 24h (which had been found sufficient to ensure equilibrium) at 25.0°C, 35.0°C, and 45.0 °C. The adsorption isotherms were studied, using similar conditions at different pH=1.0, 2.0, and 3.0.

2.6. Metal ion-uptake by zeolitic tuff using column experiment.

Glass column of 150 mm length and 10 mm inner diameter was used in this experiment. The column was packed with 1.00g ± .0001g of zeolitic tuff, a sample volume of 50.0 ml containing U(VI) or Th(IV) of 1000ppm was passed through the column at a flow rate of 1.0 ml/ 2min. The eluate was collected in a 50 ml volumetric flask, and concentration of the metal ion was then determined by using UV-VIS.

2.7. Desorption studies.

Desorption of the U(VI) and Th(IV) was carried under column condition, where zeolitic tuff was loaded with each metal ion as described in (section 3.6). A 50.0 ml of the following four eluting agents, 0.1N and 0.01N HNO_3, 0.1N H_2SO_4, 0.1 to $1*10^{-4}$ N EDTA, and 0.1N CH_3COONa were used for metal ion recovery from adsorbed zeolitic tuff, keeping the flow rate of elution at 1 ml/2min. The concentration of metal ion in the eluate was collected in five 10 ml portions, and then determined using UV-VIS.

3. Results and Discussion

3.1. Characterization of the zeolitic tuff sample.

The obtained zeolitic tuff was characterized by Fourier transform infrared (FTIR) spectroscopy, Thermogravimetric analysis (TGA) and X-ray powder diffraction (XRD) technique.

3.2. Fourier transform infrared (FTIR).

The structural information of the zeolite tuff was obtained by FTIR spectroscopy Figure (1) shows H-bonded O-H stretching at 3443.9 cm^{-1}, H_2O bending at 1640.7 cm^{-1}, 1428.6 cm^{-1} asymmetric stretching vibrations of the carbonate in the sample, 1019.1 cm^{-1} strong band due to phillipsite symmetric stretching vibration of silicate group, 610.2 cm^{-1} symmetric stretching vibration of silicate group for forsterite and 450.6 cm-1 bending vibrations for phillipsite. Calcite and forsterite are normally present in Jordanian zeolitic tuff.

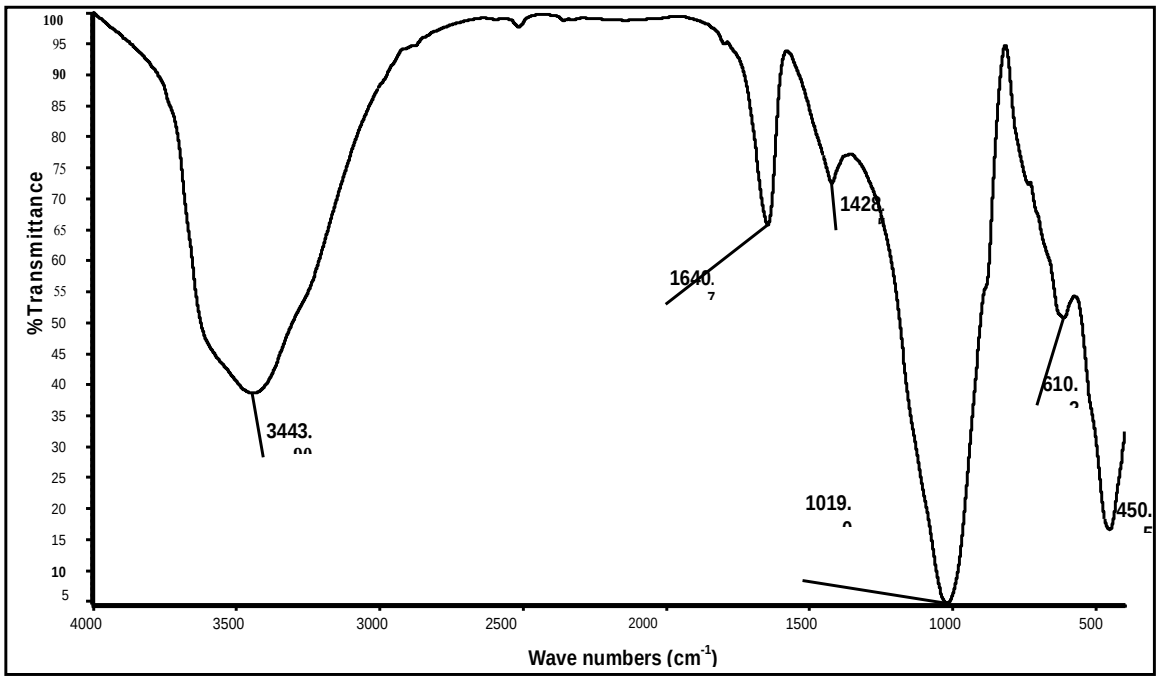

Figure (1): The FTIR spectrum of zeolitic tuff at 25ºC.

3.3. Thermal properties.

Thermal behavior of zeolitic tuff was investigated by using TGA. The TGA thermogram is given in Figure (2). The temperature ranges are 45-400, 400-800 and 800-1000°C corresponding to the loss of external, loosely bound and tightly bound water, respectively. The weight losses were found as 8.64, 3.89 and 13.93% by weight for the external, loosely and tightly bound water for the examined zeolitic tuff (Duvarcı et al., 2006). The 800-1000°C could be also related to the loss of CO_2 as a result of decarbonation of calcite.

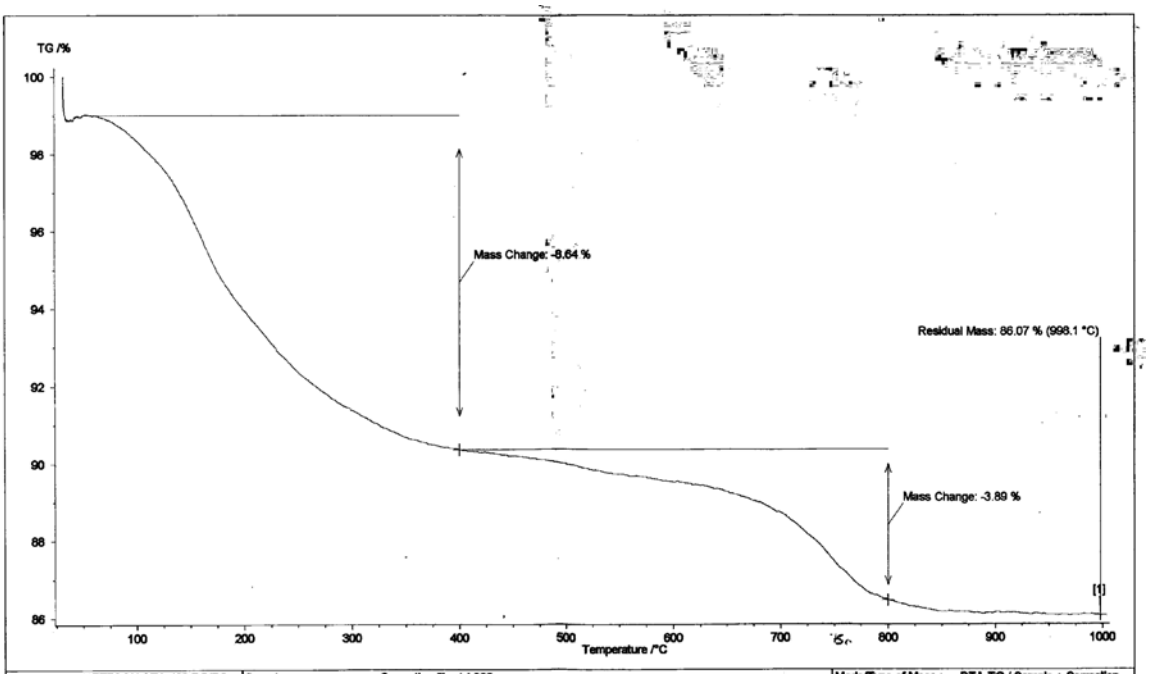

Figure (2): TGA thermogram of zeolitic tuff.

3.4. X-ray powder diffraction analysis.

The X-ray diffraction results have indicated that the examined zeolitic tuff sample is rich in Phillipsite and Chabazite together with calcite and forsterite; the XRD chart is shown in Figure (3).

3.5. Rate of metal ion sorption by zeolitic tuff

The rate of metal ions uptake by zeolitic tuff was determined at different time (0.25, 0.5, 1.0, 2.0, 4.0, 6.0, 18.0 and 24 hr), with three concentrations (5, 10, 35 ppm) at different pH (1.0, 2.0 and 3.0) and 25 °C.

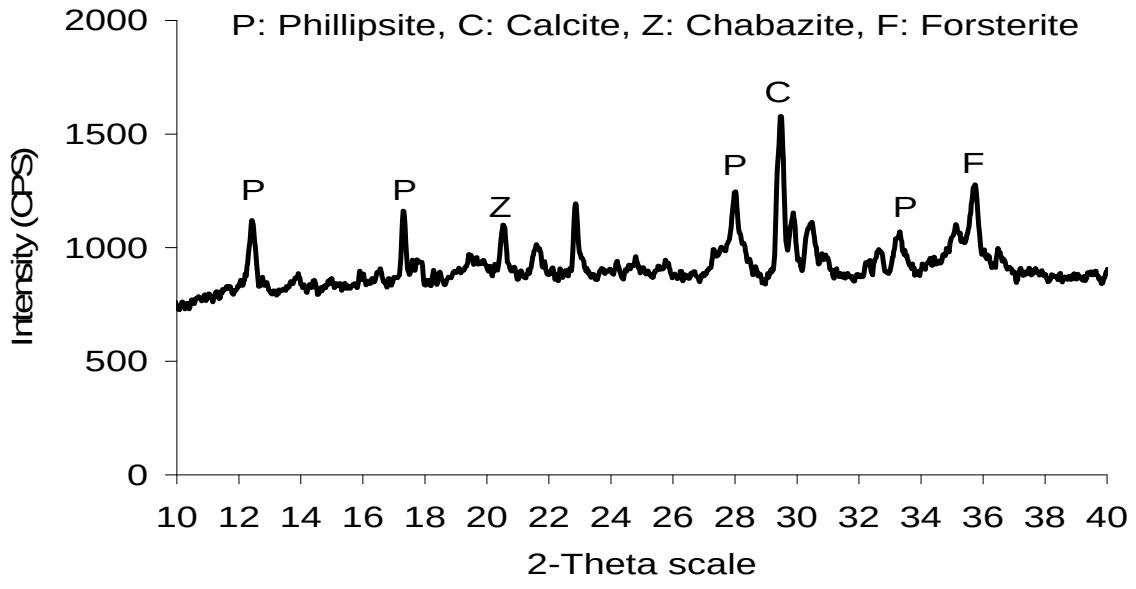

Figure (3): X-ray powder diffraction chart.

Samples of these results are shown in Figures (4 -5). Shaking for 24h has been found sufficient to ensure equilibrium for all the experiments.

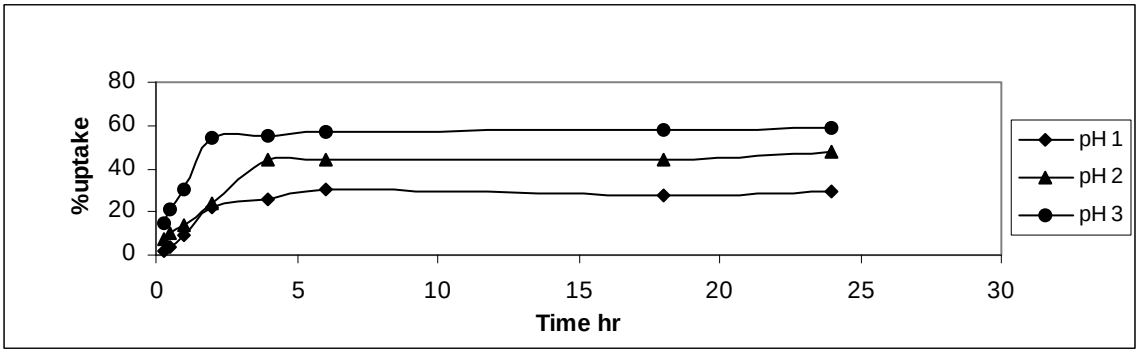

Figure (4): Thorium (IV) percentage uptake by zeolitic tuff at pH 1.0, 2.0 and 3.0 at 25°C and concentration 35ppm.

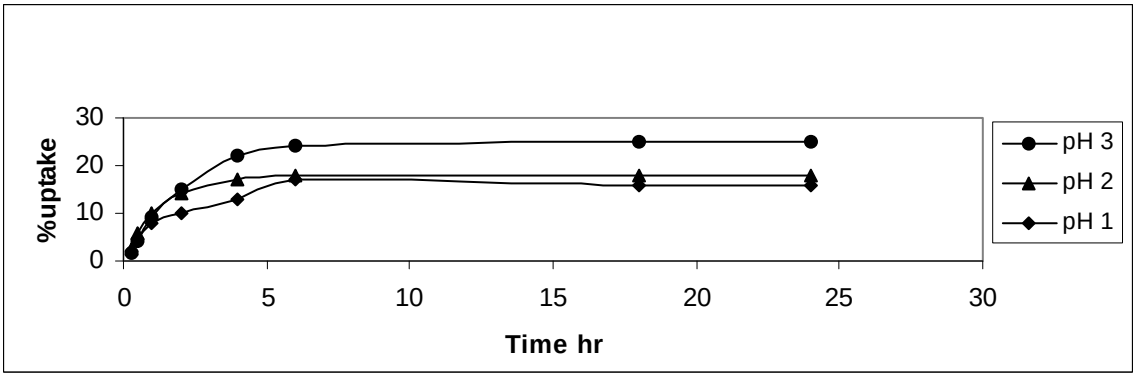

Figure (5): Uranium (VI) percentage uptake by zeolitic tuff at pH 1.0, 2.0 and 3.0 at 25°C and concentration 35 ppm.

3.6. Pseudo-second-order reaction kinetic.

Adsorption data was evaluated according to the Pseudo second-order reaction kinetic

proposed by Ho and McKay (1998):

$$dq_t/dt = k_2(q_e - q_t)^2 \quad (4)$$

where k_2 is the second order reaction constant. If Eq. (4) is integrated, the following expression is obtained:

$$1/(q_e - q_t) = k_2 t + C_2 \quad (5)$$

In Eq. (5), C_2 is the integration constant of the second order reaction kinetic. Applying the

initial condition $q_t = 0$ at $t = 0$ we get $C_2 = 1/qe$ and on elementary rearrangement this equation can be written as

$$t/q_t = 1/k_2 q_e^2 + t/q_e \quad (6)$$

In this study, the initial Thorium (IV) and Uranium(VI) concentrations were determined as 5, 10, 35 ppm . The dependences of these concentrations against time are shown in Fig. 4 and 5 for Thorium (IV) and Uranium (VI) at 25°C and pH = 3 as an example.

For both metals, the curves in the plot of t/q_t against t are linear and k_2 rate constants can be calculated from the slope of these curves as shown on figures (6-7).

The values of q_e, calculated are found from the intersection points of the second order reaction kinetic curves.

Table1. Presents all the data at different pH (1.0,2.0 and 3.0) and 25 °C.

Since the difference between q_e calculated and q_e experimental values is very small and the correlation coefficient (R^2) values for the second order reaction equation plots are high, it is seen that the Thorium (IV) and Uranium (VI) removal by zeolitic tuff is well described by the second order reaction kinetic.

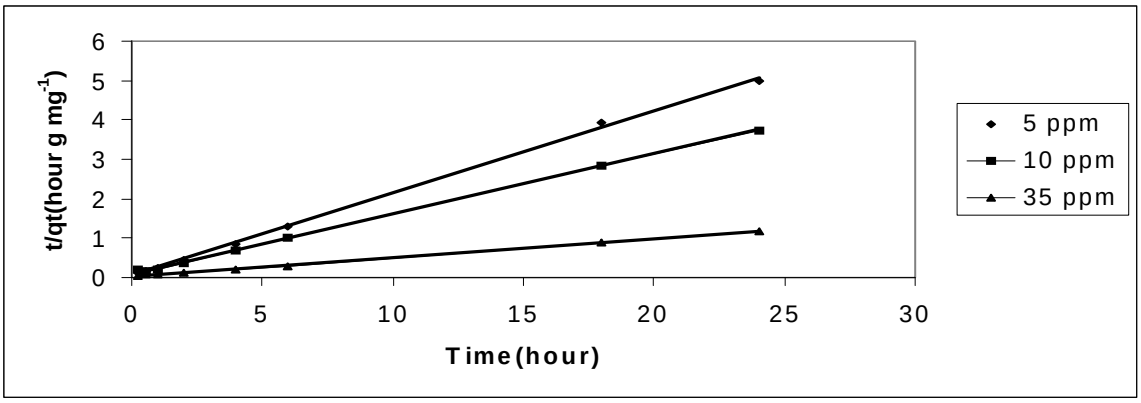

Figure (6): Pseudo-second order sorption kinetics of Thorium(IV) onto zeolitic tuff at various initial concentrations at 25°C and pH = 3 .

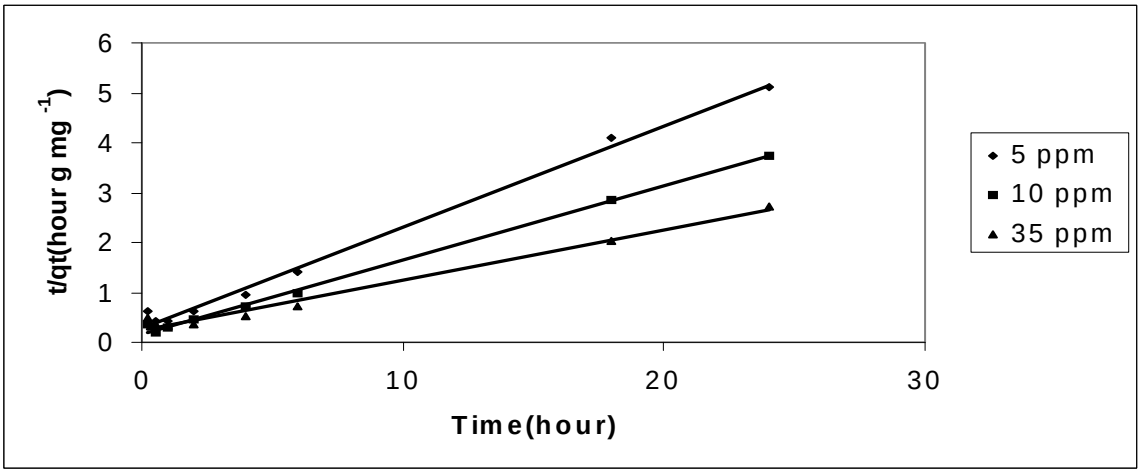

Figure (7): Pseudo-second order sorption kinetics of Uranium (VI) onto zeolitic tuff at various initial concentrations at 25°C and pH = 3.

Table (1): Adsorption rate constants, calculated q_e, experimental q_{exp} and R^2 values for the second order reaction kinetics of removal of Uranium and Thorium by natural clay at pH = 1, 2, 3 and 25 °C.

Initial metal concentration (mg/L)	Pseudo-second order pH = 1			Pseudo-second order pH =2			Pseudo-second order pH =3		
Thorium(IV)	k_2 (g/mg min)	q_e(mg/g) (q_{exp}(mg/g))	R^2	k_2 (g/mg min)	q_e(mg/g) (q_{exp}(mg/g))	R^2	k_2 (g/mg min)	q_e(mg/g) (q_{exp}(mg/g))	R^2
5 ppm	0.14	4.6 4.3	0.99	0.34	4.8 4.6	0.98	0.79	4.8 4.8	0.99
10 ppm	0.05	7.7 7.0	0.97	0.08	7.8 7.8	0.99	0.29	6.5 6.4	0.97
35 ppm	0.04	11.1 10.0	0.99	0.03	17.7 16.8	0.99	0.07	21.2 20.7	0.99
Uranium(VI)									
5 ppm	0.14	2.8 2.5	0.96	0.18	4.1 3.8	0.98	0.14	4.9 4.7	0.99
10 ppm	0.20	4.2 3.9	0.99	0.44	4.8 4.8	0.99	0.13	6.7 6.4	0.99
35 ppm	0.14	6.0 5.6	0.99	0.17	6.6 6.3	0.99	0.04	9.9 8.8	0.98

3.7. Adsorption isotherms.

3.7.1. Langmuir isotherm.

Langmuir isotherm models the single coating layer on adsorption surface. This model supposes that the adsorption takes place at a specific adsorption surface. The attraction between molecules decreases as they are getting further from the adsorption surface (Ünlüa and Ersoz, 2006). Langmuir isotherm can be defined according to the following formulas:

$$q_e = V_m K C_e / (1 + kC_e) \quad (7)$$

Where q_e is the amount of adsorbed heavy metal per unit clay mass (mg/g), V_m is the monolayer capacity, K is the equilibrium constant and C_e is the equilibrium concentration of the solution in (ppm).

Eq. (7) can be written in the following linear form:

$$C_e / q_e = 1/KV_m + C_e / V_m \quad (8)$$

The results obtained from the empirical studies were applied to Langmuir isotherm.

The plot of the linear form of Langmuir equation for Thorium (IV) and Uranium (VI) adsorption on zeolitic tuff is shown in Figures (8-9) as an example, and the values for K and V_m are shown in Tables (2-3).

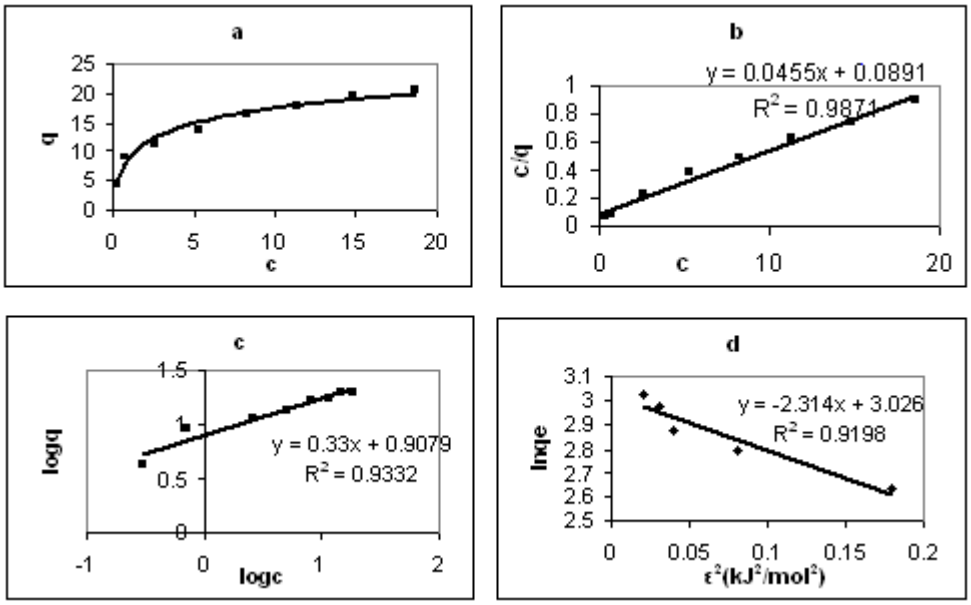

Figure (8): Plot of (a) adsorption isotherm of Th(IV), (b) linearized Langmuir (III), (c) linearized Freundlich (d) D-R at pH=3 and 25°C.

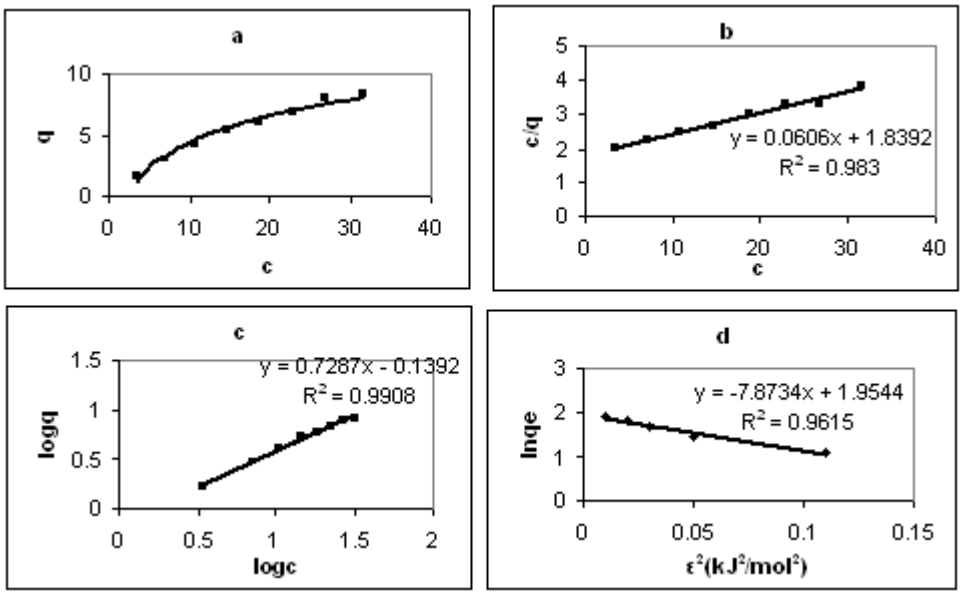

Figure (9): Plot of (a) adsorption isotherm of U(VI), (b) linearized Langmuir (III), (c) linearized Freundlich (d) D-R at pH=3 and 25°C.

3.8. Freundlich isotherm.

Freundlich isotherm (Freundlich, 1932) is used for modeling the adsorption on heterogeneous surfaces. This isotherm can be explained by the following equation:

$$q_e = K_f C_e^{1/n} \quad (9)$$

where K_f is the Freundlich constant (mg/g), and 1/n is the adsorption intensity:

The linear form of the Eq. (9) can be written as:

$$\log q_e = \log K_f + 1/n \log C_e \quad (10)$$

It is seen that the Freundlich isotherm curves are linear both in Thorium(IV) and Uranium(VI) adsorption. The Freundlich constant K_f and adsorption intensity 1/n for Thorium(IV) and Uranium(VI) are calculated from the slopes of these curves (Tables 2-3).

3.9. Dubinin–Radushkevich (D–R) isotherm.

Langmuir and Freundlich isotherms are insufficient to explain the physical and chemical characteristics of adsorption. Dubinin and Radushkevich (1947) isotherm is commonly used to describe the sorption isotherms of single solute systems. In previous studies, D–R isotherm was used to express the adsorption processes of bentonite (S. Tahir, and R. Naseem, 2006). The D–R isotherm, apart from being analogue of Langmuir isotherm, is more general than Langmuir isotherm as it rejects the homogeneous surface or constant adsorption potential (Kilislio˘glu and Bilgin, 2003).

The D–R isotherm is expressed as:

$$\ln q_e = \ln V_m - K'\varepsilon^2 \quad (11)$$

Where q_e is the heavy metal amount (mg/g) that is removed per unit clay mass, V_m is the D–R adsorption capacity (mg/g), K' is the constant related with adsorption energy (mol^2/kJ^2), and ε is the Polanyi potential.

The Polanyi potential ε can be given as (Polanyi, 1963):

$$\varepsilon = RT \ln(1 + 1/C_e) \quad (12)$$

Where R is the gas constant (kJ K^{-1} mol^{-1}), and T is the temperature (K).

The main energy of adsorption (E) is calculated by using the following formula:

$$E = (2K')^{-0.5} \quad (13)$$

Where E gives information about the physical and chemical features of adsorption.

The D–R isotherm is applied to the data obtained from the empirical studies. A plot of

$\ln q_e$ against ε^2 is given in Figures (8-9). As it is seen in Figures (8-9), the D–R plot yields a straight line.

In the D–R isotherm, adsorption capacities (V_m), adsorption energy constants (K') and the main adsorption energies (E) are calculated for Thorium(IV) and Uranium(VI) removal.

All of the isotherm model parameters for the adsorption of Thorium(IV) and Uranium(VI) are provided in Tables (2-3).

Table (2): The R^2, q_m, K_L, K_F and n values obtained from Langmuir (L), Freundlich (F) and Dubinin-Raduskevich (D-R) plots for Thorium(IV).

			L		F			D-R				
pH	T °C	R^2	q_m (mg/g)	K_L (L / mg)	R^2	K_F	n	K'(mol^2 /kJ^2)	V_m (mg/g)	E (kJ/mol)	R^2	K_d (mL/g)
1.0	25	0.9515	17.0	0.17	0.9777	4.22	2.69	0.2451	10.85	1.43	0.9684	840
	35	0.9455	14.0	0.14	0.9559	3.50	2.88	-	-	-		680
	45	0.9251	13.5	0.12	0.9578	3.08	2.74	-	-	-		450
2.0	25	0.9614	21.0	0.59	0.9185	8.16	3.60	0.0632	16.5	2.81	0.8703	940
	35	0.9753	18.8	0.62	0.9118	7.49	3.37	-	-	-	-	900
	45	0.9258	17.7	0.34	0.9258	6.64	3.58	-	-	-	-	520
3.0	25	0.9871	21.9	0.51	0.9332	8.09	3.03	0.0967	16.49	2.27	0.7962	980
	35	0.9790	19.4	0.46	0.9123	7.49	3.37	-	-	-		930
	45	0.9520	18.1	0.41	0.9753	7.42	3.87	-	-	-		600

Table (3): The R^2, q_m, K_L, K_F and n values obtained from Langmuir (L), Freundlich (F) and Dubinin-Raduskevich (D-R) plots for Uranium(VI).

			L		F			D-R				
pH	T °C	R^2	q_m (mg/g)	K_L (L / mg)	R^2	K_F	n	K'(mol^2 /kJ^2)	V_m (mg/g)	E (kJ/mol)	R^2	K_d (mL/g)
1.0	25	0.8342	10.8	0.04	0.9737	0.72	1.66	2.4956	8.16	0.45	0.939	400
	35	0.9918	8.3	0.06	0.9894	0.72	1.69	-	-	-	-	340
	45	0.9858	5.3	0.08	0.9859	0.56	1.85	-	-	-	-	270
2.0	25	0.9481	15.0	0.05	0.9964	1.05	1.55	2.3345	6.86	0.46	0.8961	440
	35	0.9219	13.0	0.04	0.9979	0.74	1.53	-	-	-		360
	45	0.9740	11.0	0.06	0.9801	0.98	1.55	-	-	-		300
3.0	25	0.9619	17.7	0.05	0.9849	1.16	1.48	3.8657	6.64	0.35	0.9615	480
	35	0.9885	17.1	0.04	0.9737	0.72	1.66	-	-	-		400
	45	0.9830	16.5	0.03	0.9908	0.73	1.37	-	-	-		320

3.10. Comparing adsorptivity between Thorium(IV) and Uranium(VI).

The correlation coefficient (R^2) values for the three types are very close, so we cannot assume that the adsorption behaviour fit one of them better, and it is a homogeneous or a heterogeneous one. Depending in the values of $\mathbf{q_m}$ and **n** in Tables (2-3), the adsorption of Thorium(IV) is more favourable than Uranium(VI) metal ions on zeolitic tuff at the same pH and temperature. The D–R isotherm showed the E values for Thorium(IV) are higher than Uranium(VI), but both values are less than 8 kJ/mol, which means that it is a physisorption process.

These observations can be explained in terms of the following two factors:

1. Hydration energy.

The adsorptivity of metal ions (q_m) on zeolitic tuff was found to be directly proportional to the ionic radius. This is due to the decrease of hydration ($-\Delta H_h$) as the ionic radius increases (Hunt, 1965). Increasing the hydration energy due to increase in the hydration shell makes it more difficult for metal ion to discharge the water of hydration. The formation of aqua complex $[M(OH_2)_m]^{n+}$ takes place (where m is larger than six, perhaps eight or nine), the aqua complex, having m H_2O molecules surrounding the central ion, has a definite structure and the cloud of water molecules (hydration shell) has another geometry than the rest of the water. Thus, when $M(NO_3)_n$ salts are dissolved in water there will be very little attraction between $[M(OH_2)_m]^{n+}$ and the solvated NO_3^- ion. Unless the other ions or ligands have a strong structure breaking influence, the sheath of water molecule will protect the metals ions from influence of other anions or ligands. When complexes are formed, the approach of a ligand will interfere with the hydration shell, and the ordered geometry will break down (Sinha, 1966). A stronger hydration shell will surround small metal ion, which has smaller radius than the metal ion with larger radius. The adsorptivity of an ion of large radius is larger than small radius.

Large charge-to-size ratio results in an increase in hydration energy, which means that the hydrated ion prefers the solution phase, where it may satisfy its hydration requirements. Ions with lower hydration energy prefer the zeolitic tuff phase. Table (4) shows that Thorium has lower hydration energy than Uranium- this means Thorium can exchange easily at the zeolitic tuff surface.

The values of electronegativity for Uranium and Thorium are shown in Table (4). Thorium(IV) is more electropositive than Uranium(VI). This means that Thorium(IV) binding onto the negative surface and q_m should be stronger and higher respectively, than Uranium(VI).

2. Hydrolysis Reaction.

Hydrolysis reaction can be represented by a hydrolysis constant (K_h)

$M^{2+} + H_2O \rightarrow MOH^+ + H^+$

From the value of K_h in Table (4), the following sequence was observed:

pK_h: $UO_2^{2+} > Th^{4+}$.

Table (4): Chemical properties of Thorium(IV) and Uranium(VI).

Metals	Th(IV)	U(VI)
Ionic radius (Å)	1.19	0.97
Electronegativity	1.30	1.38
Hydrolysis constant at 0.1M $NaClO_4$ (pK_h)	4.00	4.69
Hydration energy (kJ / mol)	-3332	-3958

This indicates that at lower pK_h value the metal ion can diffuse easily and has a stronger binding strength at the zeolitic tuff surface. Thorium(IV) has a lower pK_h, so a lower resistance to reach the active sites. As a conclusion: the binding strength of $Th^{4+} > UO_2^{2+}$ at the zeolitic tuff surface due to the hydration and hydrolysis behavior.

3.11. Effect of pH.

Tables 2 & 3 show that as the pH increases the q_m values increase for Thorium(IV) and Uranium(VI). This can be explained by the following:

In solutions of pH less than 3, Thorium shows a small tendency to hydrolyze, and the exchangeable Thorium ion (Th^{4+}) dominates. In pH 3 and greater, mononuclear (e.g., $[ThOH]^{3+}$, $[Th(OH)_2]^{2+}$ and $[Th(OH)_3]^+$) as well as polynuclear-polymeric (e.g., $[Th_2(OH)_2]^{6+}$) hydrolysis

products of the general type $[Th_x(OH)_Y]^{(4x-y)+}$ are formed. The hydroxyl number of these species depends on the Thorium concentration and rises rapidly with increasing pH. Most of the hydrolysis species can be exchanged or adsorbed on the zeolitic tuff. Thorium(IV) is the least hydrolyzed tetrapositive ion when compared with other tetrapositive actinides. In the case of uranium, the uranyl ion $(UO_2)^{2+}$ is the most dominant species in low pH solutions and Uranium uptake is mainly due to uranyl ion adsorption.

The radius of the hydrated uranyl cation can be assigned to determine how closely the centers of two ions actually approach each other in solid substances, and then to assume that such a distance is equal to the sum of the radii of the two ions. Theoretically, a rough estimation of the ionic radius of a complex ion ML_n is given as the sum of the ionic radius of the cation M and the mean diameter of the ligand L. Since the ionic radius of the uranyl ion is equal to 1.8 Å and the atomic radii of oxygen and hydrogen are 0.74 A° and 0.37 Å respectively, a rough estimation of the hydrated uranyl ion diameter gives a result higher than 6.5 Å. The estimated size of hydrated uranyl cation $[UO_2(H_2O)_5]^{2+}$ is much greater than the mean dimension of the zeolitic tuff channels; therefore the uranium (VI) attenuation by natural zeolitic tuff cannot be attributed to the cation exchange mechanism (Krestou et al. 2003). Hydrolysis of the uranyl ion practically begins at pH 3 and mononuclear (e.g., $[UO_2(OH]^+$) as well as polynuclear (e.g., $[(UO_2)_2(OH)_2]^{2+}$, $[(UO_2)_3(OH)_5]^+$) hydrolysis products of the general type $[UO_2)_x(OH)_y]^{(2x-y)+}$ are formed. The occurrence of species such as $U_2O_5^{2+}$, $U_3O_8^{2+}$ and polymeric species of the type $UO_2(UO_3)_n^{2+}$ has also been suggested. The $(UO_2)^{2+}$ hydrolysis products can be adsorbed on zeolitic tuff. However, the formation of phases such as $UO_2(OH)_2$, which can be precipitated, is also possible. The metal species, present in the aqueous solutions, strongly depend on the pH.

The adsorption of some species by ion exchange processes can be considered to take place at the microporous minerals (zeolitic tuffs, clay minerals and micas). Where individual metal species penetrate into the lattice through the micropores and replace exchangeable ions (mainly Na^+ and K^+) but adsorption (surface uptake) takes place both on the microporous and the non-microporous minerals (feldspars, SiO_2 phases) (Misaelides et al., 1995).

In Zeolitic tuff, the silanol (> Si-OH) and Aluminol (> Al-OH) groups are formed on the edge surface of the material. Depending on the solution pH, these groups behave as basic or acidic solutions according to the following reactions:

$> MOH^0 + H^+ \leftrightarrow MOH_2^+$ in acidic solutions.

$> MOH^0 + OH^- \leftrightarrow MO^- + H_2O$ in basic solutions.

The Uranium(VI) and Thorium(IV) species are preferably adsorbed on the silanol groups, which are not protonated at pH equals 3 rather than on the aluminol groups, and which are strongly protonated in the same pH region (Talip et al., 2008).

$> SiOH^0 + UO_2^{2+} \rightarrow [> SiO\text{-}UO_2]^+ + H^+$

$> SiOH^0 + Th^{4+} \rightarrow [> SiO\text{-}Th]^{3+} + H^+$

So as the pH increases the amount of deprotonated SiOH increases. Therefore, the negative charge on the surface increases, and the adsorbed metal ions increase.

3.12. Effect of temperature.

From the data in Tables (2&3), the relation $\ln K_d$ vs. 1/T was plotted and from the van't Hoff equation, ΔH and ΔS were calculated for Th(IV) and U(VI) as shown in Table (5). The adsorptivity process is enthalpy and entropy driven for Thorium(IV) and Uranium(VI). The negative values of enthalpy show that the sorption of Thorium(IV) and Uranium(VI) on zeolitic tuff is an exothermic process. Values of the free energy (ΔG) of adsorption for the adsorption of Thorium(IV) and Uranium(VI) on zeolitic tuff are negative, showing that adsorption processes are spontaneous in nature.

Table (5): Enthalpy, entropy and free energy (298 K) values for the adsorption of Thorium(IV) and Uranium(VI) on zeolitic tuff.

Metal	Th(IV) pH=1	Th(IV) pH=2	Th(IV) pH=3	U(VI) pH=1	U(VI) pH=2	U(VI) pH=3
ΔH(kJ/mol)	-23.8	-22.7	-18.9	-14.7	-14.6	-15.1
ΔS(J/mol.K)	-23.7	-18.5	-5.6	0.4	1.1	0.6
ΔG (kJ/mol)	-16.7	-17.2	-17.1	-14.6	-14.3	-14.9

3.13. Column Experiments.

3.14. Metal Ion Uptake by Zeolitic tuff.

The metal ion uptake by zeolitic tuff using column experiment for Thorium(IV) and Uranium(VI) were determined at pH= 3, 25°C, initial concentration of 1000 ppm and a flow rate of 1 ml /2 min. The percent uptake for metal ions is represented in Table (6).

Table (6): Metal ion uptake using column experiment at pH= 3, 25°C.

Metal Ion	C_i (ppm)	Final concentration (ppm)	Loaded concentration (ppm)	% Uptake
Thorium(IV)	1000	69.0	931	93.1
Uranium(VI)	1000	118.0	882	88.2

It can be seen that the uptake capacities of the metal ions fall in the order Th(IV) > U(VI).

3.15. Desorption studies.

A four eluting agents, 0.1N HNO_3, 0.1 H_2SO_4, 0.1-$1*10^{-4}$N EDTA (pH= 3.0), and 0.1N CH_3COONa were used for removal of metal ions, keeping the flow rate of elution at 1 ml /2 min. The eluate was collected in five portions, 10 ml each; the results are expressed as percent recovery and represented in Tables (7& 8).

Depending on the values of percentage of accumulative recovery, in Table (7) and Table (8), the following trend was observed for the eluting agents of Th(IV) from zeolitic tuff:

$1*10^{-4}$N EDTA > 0.001N EDTA > 0.01 N EDTA > 0.1N HNO_3 > 0.1N CH_3COONa

Table (7): Desorption of Th(IV) ions from zeolitic tuff.

Eluting agents	%Recovery first portion	%Recovery second portion	%Recovery third portion	%Recovery fourth portion	%Recovery fifth portion	%Cumulative recovery
0.1N HNO_3	4.0	3.5	3.5	1.9	1.7	14.6
0.1N H_2SO_4	–	–	–	–	–	–
$1*10^{-4}$N EDTA	11.0	8.5	8.3	7.6	5.4	40.8
0.1N EDTA	-	-	-	-	-	-
0.01N EDTA	4.3	3.7	3.6	3.6	3.2	17.5
0.001N EDTA	8.9	7.2	5.1	2.3	1.5	25.0
0.1N $NaC_2H_3O_2$	7.1	2.9	0.4	0.0	0.0	10.4

Table (8): Desorption of U(VI) ions from zeolitic tuff.

Eluting agents	%Recovery first portion	%Recovery second portion	%Recovery third portion	%Recovery fourth portion	%Recovery fifth portion	%Cumulative recovery
0.1N HNO_3	10.5	8.5	2.9	2.9	2.3	27.1
0.1N H_2SO_4	10.5	7.9	5.4	2.8	2.8	29.4
$1*10^{-4}$N EDTA	8.0	5.2	3.5	3.0	2.0	21.7
0.1N EDTA	-	-	-	-	-	-
0.01N EDTA	2.3	2.1	1.7	0.5	0.3	6.9
0.001N EDTA	5.7	3.9	2.4	1.2	0.7	13.9
0.1N $NaC_2H_3O_2$	9.1	7.3	4.2	3.6	3.3	27.5

While the following trend was observed for eluting agents of U(VI) from zeolitic tuff:

0.1N H_2SO_4 > 0.1N CH_3COONa > 0.1N HNO_3 > $1*10^{-4}$N EDTA >0.001N EDTA > 0.01 N EDTA.

It can be noticed that the best desorption for Th(IV) was observed for $1*10^{-4}$N EDTA, but the best desorption for U(VI) was observed for 0.1N H_2SO_4.

Desorption yield for zeolitic tuff decreased with increasing the desorption stages (Akyil and Yusan, 2008). When concentration of EDTA is increased, desorption of Uranium(VI) and Thorium(IV) decreased. Thorium sulfate precipitated in the column (K_{sp} =$9.6*10^{-15}$) while Uranium(VI) form two successive soluble complexes with sulfate

$UO_2^{2+} + SO_4^{2-} = UO_2SO_{4\,(aq)}$ (14)

$UO_2^{2+} + 2SO_4^{2-} = UO_2(SO_4)_2^{2-}{}_{(aq)}$ (15)

Stability constant (logβM) for equation (14) equal 1.96 ± 0.06 but stability constant(logβM) for equation (15) equal 2.97 ± 0.03 (Tian and Rao, 2008).

4. Conclusion

The used size fraction (250-500 μm) of Tulul al-Shabba zeolitic tuff from Jordan is dominated by phillipsite and chabazite. The sorption behavior of the used samples towards Uranium(VI) and Thorium$(IV)^+$ metal ions has indicated high initial rate of metal ions uptake. This study recommends the use of Jordanian zeolitic tuff to remove Uranium(VI) and Thorium(IV) from acidic solution in the expected mining or purification processes. Further work should be carried to enhance the desorption of Uranium(VI) and Thorium(IV) from zeolitic tuff.

References

[1] Akyil, S., and Yusan, S., 2008. Sorption of Uranium (VI) from Aqueous Solutions by Akaganeite, Journal of Hazardous Materials, 160: 388-395.

[2] Ali, A., and El-bishtawi, R., 1997. Removal of Lead and Nickel Ions Using Zeolite, J. of Chem. Tech. Biotech, 69: 27-34.

[3] Dubinin, M. M., L. V. Radushkevich., and Dokl. Ak., 1947. A Theoretical Isotherm for Adsorption on Heterogeneous Surface, Nauk SSSR, 55: 331- 333.

[4] Duvarcı, Ö., Akdeniz, Y., ÖzmıhÇı, F., Űlkű, S., BalkÖse., and M. Ċiftċioğlu, M., 2006. Thermal Behavior of a Zeolitic Tuff, Ceramics International, 33: 795-801.

[5] Eral, T Z., and Hicsonmez, M. U., 2008. Adsorption of Thorium from Aqueous Solutions by Perlite, Journal of Environmental Radioactivity, 2: 1-5.

[6] Fendorf, S.E., and Li, G., 1996. Kinetics of Chromate Reduction by Ferrous Iron, Environ. Sci. Technol, 30: 1614-1617.

[7] Freundlich, H., 1932. Of the adsorption of gases. Section II. Kinetics and energetics of gas adsorption. Introductory paper to section II, Trans, Faraday Soc, 28: 195 - 201.

[8] Harvey, D. 2000. Modern analytical chemistry. 1st Ed., McGraw-Hill, U.S.A.

[9] Ho, Y.S., and McKay, G., 1998. Sorption of Dye from Aqueous Solution by Peat, J.

[10] Chem. Eng, 70: 115–124.

[11] Hunt, J.P.1965. Metal Ions in Aqueous Solutions. 2nd Ed., Benjamin Inc, New York.Kaygun, A., and Akyil, S., 2007. Study of the Behavior of Thorium Adsorption on PAN / Zeolite Composite Adsorbent, Journal of Hazardous Materials, 147: 357-362.

[12] Khaled, M. M., and Khalili, F.I., 1999. Solvent Extraction of Uranium(VI) by Didodecylphosphoric acid, Science and Technology, 4: 15-21.

[13] Khalili, F., Al-Taweel, S.A., Yousef, Y.Y., and Al-Tarawneh, S.A., 2008. Synthesis, Characterization and Solvent Extraction Properties of New Thiophene Based Trifluoromethyl-Substituted β-Diketones for Thorium (IV) and Uranium (VI) Ions, Journal of Saudi Chemical Society, 12(2): 165-176.

[14] Khoury, H., Ibrahim, K., Ghrir, A., and Ed-Deen, T. 2003. Zeolites and zeolitic tuff in Jordan. Published by the University of Jordan, amman - Jordan.

[15] Khoury, H. 2006. Industrial rocks and minerals in Jordan. 2nd Ed., Published by the University of Jordan, Amman - Jordan.

[16] -Kilislio˘glu, A., and Bilgin, B., 2003. Thermodynamic and Kinetic Investigation of Uranium Adsorption on Amberlite IR-118-H Resin, Appl. Radiat. Isot, 50: 155 - 170.

[17] Konodo, K., Momoto, K., and Nakashio, T., 1989. Equilibrium of Solvent Extraction of Lanthanides with Didodecylphosphoric, Solvent Extraction and Ion Exchange, 7(6): 1027-1041.

[18] Krestou, A., Xenidis, A., and Panias, D., 2003. Mechanism of Aqueous Uranium(VI) Uptake by Natural Zeolite Tuff, Minerals Engineering, (16):1363-1370.

[19] Lazaridis, K., Peleka, N., Karapantsios, D., and Matis, A., 2004. Copper Removal from Effluents by Various Separation Techniques, Hydrometallurgy, 74: 149-156.

[20] Lee, D.C., Park, C.J., Yang, J.E., Jeong, Y.H., and Rhee, H.I., 2000. Screening of Hexavalent Chromium Biosorbent Marine Algae, Biotechnol, 54: 445-448.

[21] Misaelides, P., Godelitsas, A., Filippidis, A., Charistos, D., and Anousis, I., 1995. Thorium and Uranium Uptake by Natural Zeolitic Materials, Sci. Total Environ, 173/174: 237-246.

[22] Nazzal, M.K. 2006. The Effect of Ionic Strength on the Extraction of U(VI) from Perchlorate, Nitrate and Phosphate Solution by Didodecylphosphoric acid(HDDPA), M. Sc.Thesis, The University of Jordan.

[23] Polanyi, M., 1963. The potential Theory of Adsorption, Science, 141: 1010 – 1013.

[24] Savvin, S. B., 1961. Analytical Use of Arsenazo(III) Determination of Thorium, Zirconium, Uranium and Rare Earth Elements, Talanta, 8: 673- 679.

[25] Sinha, S.P. 1966. Complexes of the Rare Earths. 1st Ed., Pergamon Press, London.

[26] Skoog, A. West, M. and Holler, F. 1994. Analytical Chemistry an Introduction. 6th Ed., John Vondeling, U.S.A.

[27] Slejko, L. 1985. Adsorption Technology. Marcel Dekker, New York.

[28] Tahir, S., and Naseem, R., 2006. Removal of a Cationic Dye from Aqueous Solution by Adsorption onto Bentonite Clay, Chemosphere, 63:1842–1848.

[29] Tian, G., and Rao, L., 2009. Spectrophotometric and Calorimetric Studies of U(VI) Complexation with Sulfate at 25C° to 70C°, J. Chem. Thermodynamics, 41: 569-574.

[30] Ünlüa, N., and Ersoz, M., 2006. Adsorption Characteristics of Heavy Metal Ions onto a Low Cost Biopolymeric Sorbent from Aqueous Solutions, J. Hazard. Mater, B136: 272–280.